Design of Hysteretic Damped Braces to Improve the Seismic Performance of Steel and R.C. Framed Structures

Fabio Mazza*, Alfonso Vulcano**

SUMMARY – *A Displacement-Based Design (D.B.D.) procedure is adopted for the retrofit of framed structures by inserting hysteretic damped braces (HYDBs) in order to attain, for a specific level of seismic intensity, a designated performance level. To check the reliability of the design procedure, two six-storey buildings are considered as having steel and r.c. framed structures, which, originally designed in a medium-risk seismic region, have to be retrofitted as if in a high-risk seismic region. To avoid high deformability of the steel structure at the damage limit state (SLD) and brittle behaviour of the r.c. structure at the life-safety limit state (SLV), two retrofitting structural solutions are examined: additional diagonal braces; HYDs supported by the additional diagonal braces. Nonlinear dynamic analyses under real ground motions are carried out by a step-by-step procedure. The frame members and the HYDs are idealized by a bilinear model; an elastic behaviour is considered for the braces.*

Keywords: Steel and r.c. framed structures, Seismic retrofitting, Hysteretic damped braces, Damage limit state, Life-safety limit state, Displacement-based design procedure, Nonlinear static and dynamic analysis.

1. Introduction

Experimental studies and many structural applications [Christopoulos and Filiatrault, 2006; Ponzo et al., 2012; Sorace and Terenzi, 2012a] have proved the effectiveness of supplementary energy dissipation to enhance the seismic performance of steel [Sorace and Terenzi, 2009; Mazza and Vulcano, 2011] and r.c. [Mazza and Vulcano, 2009; Ponzo et al., 2010; Sorace and Terenzi, 2012b] framed structures. The supplementary damping devices can be classified as: displacement-dependent (e.g. hysteretic damper, HYD), velocity-dependent (e.g. viscoelastic damper, VED) and self-centring (e.g. shape memory alloys damper, SMAD). For a widespread application of the damped braces practical and reliable design procedures are needed. According to the Performance-Based Design [Bertero, 2002], the coupling of a performance level (e.g. operational, damage, life-safety or collapse) with a specific level of ground motion intensity (e.g. frequent, occasional, rare or very rare) provides a performance design objective.

A design procedure for steel braces equipped with HYDs was proposed by the authors [Mazza and Vulcano, 2008, 2013], following a Displacement-Based Design (D.B.D.) approach in which the design starts from a target deformation [Priestley et al., 2007]. In the present work, to check the effectiveness of the design procedure, a numerical investigation is carried out by investigating the nonlinear seismic response of two six-storey buildings, with a steel or a r.c. framed structure. These structures, originally designed according to an old Italian seismic code [DM96, 1996] for a medium-risk zone, are supposed to be retrofitted by the insertion of hysteretic damped braces (HYDBs) to attain performance levels imposed by the current Italian seismic code [NTC08, 2008] in a high-risk zone. To avoid high deformability of the steel structure, at the damage limit state (SLD), and brittle behaviour of the r.c. structure, at the life-safety limit state (SLV), braced frame (BF) and damped braced frame (DBF) retrofitting structural solutions are examined.

2. Displacement-Based Design of Damped Braces

A proportional stiffness criterion, which assumes, at each storey, the same value of the stiffness ratio K^*_{DB} (= K_{DB}/K_F, K_{DB} being the lateral stiffness of the damped braces and K_F that of the unbraced frame), is combined with the D.B.D. method. The stiffness of a damped brace, K_{DB}, can be expressed as for an in-series model depending on the brace stiffness, K_B, and the elastic stiffness of the damper, K_D:

$$K_{DB} = \frac{1}{1/K_B + 1/K_D}. \tag{1}$$

* Dipartimento di Ingegneria Civile, Università della Calabria, Rende, Cosenza, ITALY, fabio.mazza@unical.it

** Dipartimento di Ingegneria Civile, Università della Calabria, Rende, Cosenza, ITALY, vulcano@unical.it

In case of HYDs, the distribution profile of the yield-load (N_y) along the structure height is assumed to be similar to that of the elastic force induced by the braces under the seismic forces (e.g. similar to those associated with the first-mode shape, neglecting the contribution of the modes with higher frequency). The main steps of the proposed design procedure are summarized below. Further details can be found in previous works by the authors [Mazza and Vulcano, 2008, 2013].

2.1. *Pushover analysis of the unbraced frame and definition of an equivalent single degree of freedom (ESDOF) system to evaluate the equivalent viscous damping due to hysteresis*

Nonlinear static (pushover) analysis of the unbraced frame (whose properties are supposed as given), under constant gravity loads and monotonically increasing horizontal loads, is carried out to obtain the base shear-top displacement ($V^{(F)}$-d) curve. For this purpose, the lowest capacity curve is selected among those corresponding to the most common lateral-load profiles: e.g. a "uniform" distribution, proportional to the floor masses (m_1, m_2, ..., m_n); a "first-mode" distribution, obtained multiplying the first-mode components $\phi_1^{(1)}$, $\phi_2^{(1)}$, ..., $\phi_n^{(1)}$) by the corresponding floor masses.

The selected $V^{(F)}$-d curve can be idealized as bilinear and the original frame can be represented by an ESDOF system [Fajfar, 1999] characterized by a bilinear curve (V^*-d^*), with a yield displacement $d_y^{(F)}$ and a stiffness hardening ratio r_F, derived from the idealized $V^{(F)}$-d curve (see Figure 1a). Once the displacement (d_p) and the corresponding base shear ($V_p^{(F)}$) are settled, for a given performance level, the ductility

$$\mu_F = d_p \big/ d_y^{(F)} \tag{2}$$

and the equivalent (secant) stiffness

$$K_e^{(F)} = V_p^{(F)} \big/ d_p \tag{3}$$

can be evaluated for the frame.

From the Jacobsen approach [Jacobsen, 1930], the equivalent viscous damping due to hysteresis of the framed structure, $\xi_F^{(h)}$, can be calculated:

$$\xi_F^{(h)}(\%) = \kappa 63.7 (\mu_F - 1)(1 - r_F) \Big/ \left[\mu_F + \mu_F r_F (\mu_F - 1)\right]. \tag{4}$$

where μ_F and r_F have been defined above. The parameter κ, which accounts for the mechanical degradation, depends on the structural type (e.g. κ can be assumed as equal to 1/3 in the case of poor structural behaviour [ATC, 1996]). It is worth noting that $\xi_F^{(h)}$ is assumed as equal to zero when $d_p \le d_y^{(F)}$.

2.2. *Equivalent viscous damping due to hysteresis of the damped braces*

If the constitutive law of the equivalent damped brace is idealized as bilinear (see Figure 1b), the corresponding viscous damping, $\xi_{DB} = \xi_{DB}(\mu_{DB},\ r_{DB})$, can be evaluated as

$$\xi_{DB}(\%) = 63.7 (\mu_{DB} - 1)(1 - r_{DB}) \Big/ \left[\mu_{DB} + \mu_{DB} r_{DB} (\mu_{DB} - 1)\right] \tag{5}$$

where μ_{DB}, and r_{DB} are, respectively, the ductility demand and the stiffness hardening ratio of the equivalent damped brace.

The ductility demand of the equivalent damped brace, μ_{DB}, can be evaluated as

$$\mu_{DB} = \left[1 + (\mu_{DB} - 1)(1 + r_D K_D^*)\right] \big/ (1 + K_D^*) \tag{6}$$

μ_D being the damper ductility, whose value should be selected to be compatible with the deformation capacity of the damper itself, r_D the stiffness hardening ratio of the damper and $K^*_D(= K_D/K_B)$ the stiffness ratio reasonably assumed as rather less than 1.

The stiffness hardening ratio of the damped brace, r_{DB}, can be expressed as

$$\begin{aligned} r_{DB} &= (1/K_B + 1/K_D) \big/ \left[1/K_B + 1/(r_D K_D)\right] = \\ &= r_D (1 + K_D^*) \big/ (1 + r_D K_D^*) \end{aligned} \tag{7}$$

where K_B, K_D, r_D and K^*_D have been defined above.

Because the Jacobsen approach leads to an overestimation of the damping due to hysteresis of the framed structure and HYDs, the equivalent viscous damping could be suitably reduced [Mazza and Vulcano, 2014].

2.3. *Equivalent viscous damping of the frame with damped braces*

Assuming a suitable value of the elastic viscous damping for the framed structure (e.g. as commonly done, $\xi_V = 5\%$), the equivalent viscous damping of the in-parallel system comprised of framed structure (*F*) and damped braces (*DBs*) is

$$\xi_e(\%) = \xi_V + \left[\xi_F^{(h)} V_p^{(F)} + \xi_{DB} V_p^{(DB)}\right] \big/ \left[V_p^{(F)} + V_p^{(DB)}\right] \tag{8}$$

where $\xi_F^{(h)}$ and ξ_{DB} have been calculated in steps 2.1 and 2.2, respectively, $V_p^{(F)}$ has been defined above and $V_p^{(DB)}$ represents the base-shear contribution due to the damped braces of the damped braced frame at the performance point. Then, with reference to the displacement spectrum for ξ_e, the effective period (T_e) of the *DBF* can be evaluated as the period corresponding to the performance displacement d_p.

2.4. *Effective stiffness of the equivalent damped brace*

Once the mass of the ESDOF system, $m_e = \sum m_i\phi_i$, is calculated, the effective stiffness of *DBF* (K_e) and the effective stiffness required by the damped braces ($K_e^{(DB)}$) can be evaluated as

$$K_e = 4\pi^2 m_e \big/ T_e^2 \tag{9}$$

$$K_e^{(DB)} = K_e - K_e^{(F)}. \tag{10}$$

2.5. *Effective strength properties of the equivalent damped brace*

Because the base shear-displacement curve representing the response of the damped braces of the actual structure ($V^{(DB)}$-d) has been idealized as bilinear, the base-shear contributions of the damped braces at the performance and yielding points ($V_p^{(DB)}$ and $V_y^{(DB)}$, respectively) can be calculated:

$$V_p^{(DB)} = K_e^{(DB)} d_p \tag{11}$$

$$V_y^{(DB)} = V_p^{(DB)} \big/ \left[1 + r_{DB}(\mu_{DB} - 1)\right]. \tag{12}$$

It is worth mentioning that the equivalent viscous damping expressed by Equation (8) depends on the base-shear $V_p^{(DB)}$, which is initially unknown. As a consequence, an iterative procedure is needed for the solution of Equations (8)-(12).

2.6. *Design of the hysteretic damped braces of the damped braced frame (DBF)*

Finally, the distribution of the lateral loads carried by the damped braces at the yielding point ($d_y^{(DB)}$) can be assumed. Once the shear at a generic storey, $V_{yi}^{(DB)}$, is calculated, the quantities which are needed for designing the damped brace at that storey can be determined. In particular, for a diagonal brace with HYD, the yield-load, N_{yi}, and the elastic stiffness of the damped brace (along the brace direction), $K_i^{(DB)}$, can be expressed as specified in Figure 1c.

3. **Steel and R.C. Test Structures**

Two typical steel-office and r.c.-residential framed buildings, whose symmetric plans are shown in Figure 2a, are considered as test structures. The geometric dimensions and size of the sections of the original frames are shown in Figure 2b, while the main dynamical properties are reported in Table 1: i.e. floor masses (m_i), horizontal displacement components of the first vibration mode $\phi_i^{(1)}$ and corresponding vibration period ($T_{1Y,DBF}$) in the *Y* ground motion direction.

Tab. 1. *Dynamical properties of the unbraced framed buildings.*
Proprietà dinamiche delle strutture intelaiate senza controventi.

Storey	Steel structure ($T_{1Y,UF}$ = 1.885s)		R.c. structure ($T_{1Y,UF}$ = 0.762s)	
	m_i [kNs²/m]	$\phi_i^{(1)}$	mi [kNs²/m]	$\phi_i^{(1)}$
6	90	1.00	171	1.00
5	154	0.84	245	0.83
4	156	0.68	257	0.63
3	157	0.52	264	0.44
2	159	0.36	285	0.26
1	163	0.20	301	0.13

Tab. 2. *Main parameters of the ESDOF system.*
Principali parametri del sistema equivalente ad un grado di libertà.

Steel structure		R.c. structure	
Γ	1.46	Γ	1.48
V_y*	585 kN	V_y*	1315 kN
V_u*	585 kN	V_u*	1315 kN
d_y*	11.8 cm	d_y*	2.9 cm
d_u*	26.0 cm	d_u*	6.5 cm
m_e	495 kN × s²/m	m_e	765 kN × s²/m
K_e	4942 kN/m	K_e	44949 kN/m

A simulated design of the original framed buildings is carried out according to the previous Italian seismic code [DM96, 1996], for a medium-risk seismic region (seismic coefficient: $C = 0.07$) and a typical subsoil class (main coefficients: $R = \varepsilon = \beta = 1$). The gravity loads for the steel (r.c.) framed structure are represented by a dead load of 3.2 kN/m² (4.2 kN/m²) on the top floor and 4.1 kN/m² (5.0 kN/m²) on the other floors, and a live load of 3.0 kN/m² (2.0 kN/m²) on all the floors; infill walls, regularly distributed in elevation along the perimeter (Figure 2a) are considered, assuming an average weight of about 0.4 kN/m² (2.7 kN/m²). Structural steel with yield strength of 355 N/mm², concrete cylindrical compressive strength of 25 N/mm² and steel reinforcement with yield strength of 375 N/mm² are considered.

The nonlinear static analysis of the steel and r.c. framed structures is carried out by the step-by-step procedure described in a previous paper [Mazza and Vulcano, 2008], assuming an elastic-perfectly plastic (e.p.p.) behaviour. Constant gravity loads and monotonically increasing horizontal loads applied at the centre of mass of each storey are considered. As done in Section 2.1, two lateral-load profiles are assumed along the building height: "uniform" profile, proportional to the floor masses; "modal" profile, proportional to the first mode shape multiplied by the floor masses. The nonlinear analysis is stopped once the ultimate value of the ductility demand is attained at some critical section of the frame members or some compressed structural member (column or brace) buckles. In particular, the ultimate values of the curvature ductility are evaluated according to the provisions of the current Italian seismic code [NTC08, 2008] for the assessment of existing buildings. The main parameters of the ESDOF system for the steel and r.c. frames are reported in Table 2.

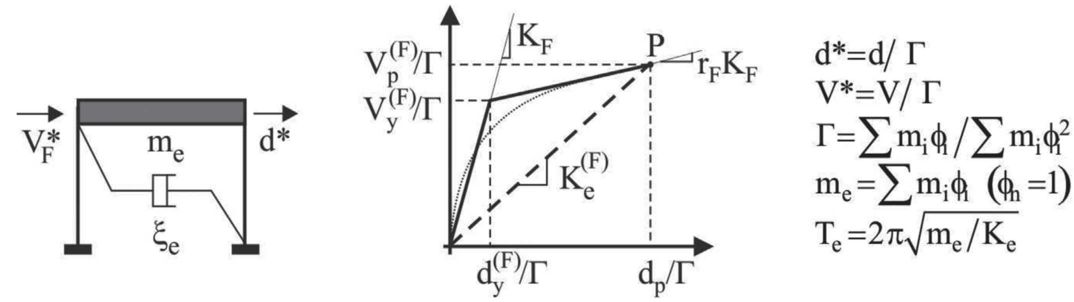

(a) Equivalent single degree of freedom of the framed structure (F)

(a) Sistema ad un grado di libertà equivalente alla struttura intelaiata (F)

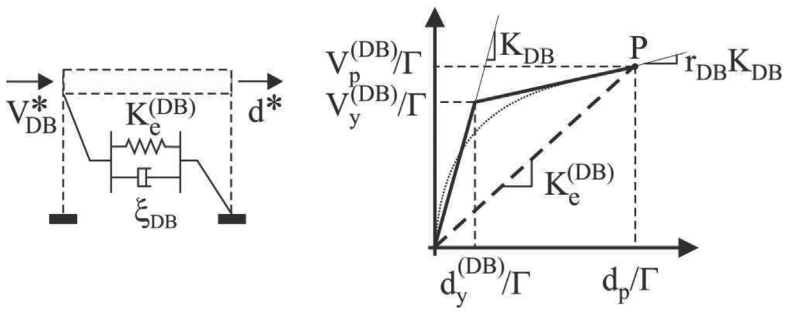

(b) Equivalent single degree of freedom of the damped braces (DBs)

(b) Sistema ad un grado di libertà equivalente ai controventi dissipativi (DBs)

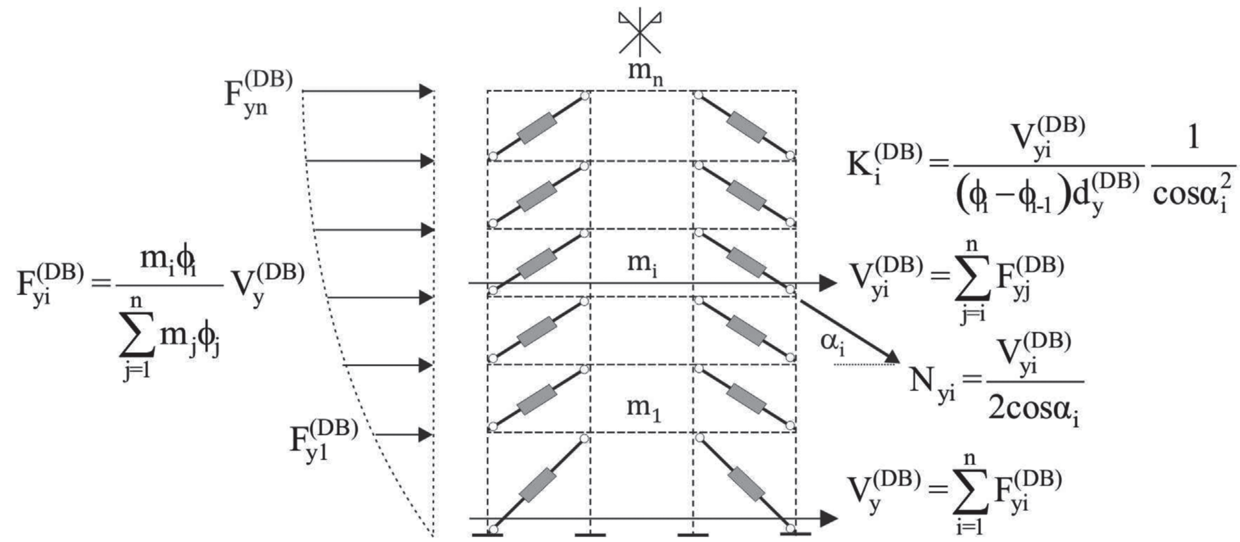

(c) Damped braced frame (DBF)

(c) Struttura intelaiata con controventi dissipativi (DBF)

Fig. 1. *Quantities for design of diagonal braces with HYDs.*
Parametri di progetto dei controventi diagonali con dissipatori isteretici (HYDs).

Finally, the capacity curve of an ESDOF system is assumed as to be the capacity curve of the original structure subjected to the load profile producing the lower strength capacity.

To upgrade the test structures from a medium-risk region to a high-risk seismic region diagonal steel braces without or with HYDs are inserted at each storey. A braced frame (BF) and a damped braced frame (DBF) are shown in Figure 3b and Figure 3c, respectively.

The design of the HYDBs is carried out according to the procedure described above, considering seismic loads provided by NTC08 for a high-risk seismic region and subsoil class B. In Table 3, the following data are reported for damage (SLD) and life-safety (SLV)

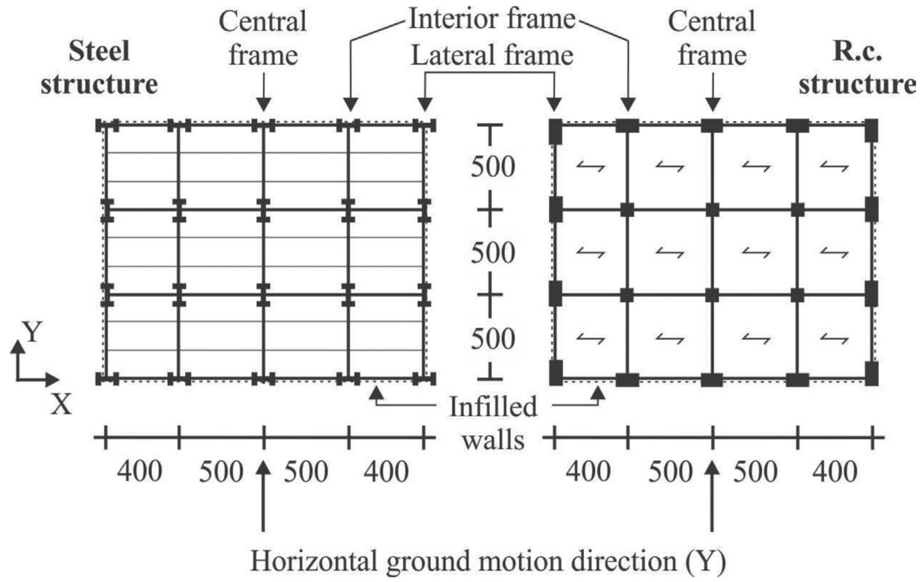

(a) Plan

(a) Pianta

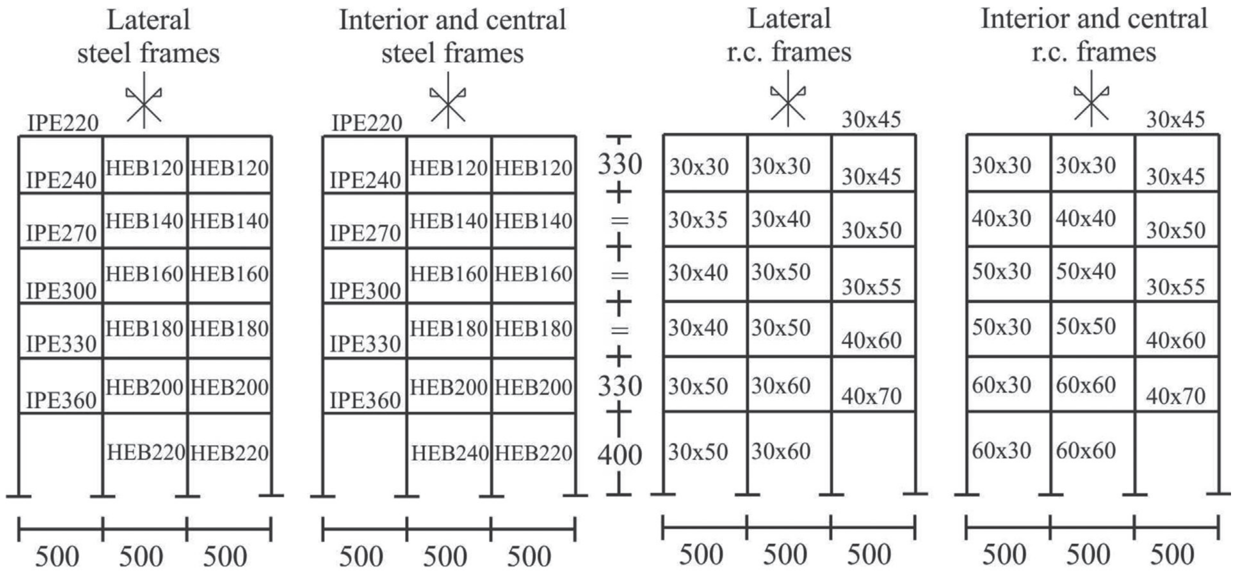

(b) Elevation (Y direction)

(b) Elevazione (direzione Y)

Fig. 2. *Layout of the steel and r.c. unbraced frames (dimensions in cm).*
Schema delle strutture intelaiate in acciaio ed in c.a. non controventate (dimensioni in cm).

limit states: peak ground acceleration on rock, a_g; return period (T_R); maximum spectrum amplification coefficient, F_0; site amplification factor, $S = S_S \cdot S_T$, S_S and S_T being factors accounting for subsoil and topographic characteristics; peak ground acceleration PGA ($= a_g \times S$) on subsoil class B.

In particular, to avoid high deformability of the steel structure, a design value of the drift ratio $\Delta / h = 0.5\%/\gamma_{SLD} = 0.42\%$, where e.g. a safety factor $\gamma_{SLD} = 1.2$, is assumed at the damage limit state (SLD); on the other hand, to avoid brittle behaviour of the r.c. structure, a design value of the frame ductility $\mu_F = 1.0{*}\gamma_{SLV} = 1.2$, where e.g. a safety factor $\gamma_{SLV} = 1.2$, is considered at the life-safety limit state (SLV). The parameters obtained in the main steps of the design procedure described above are summarized in Tables 4-9, distinguishing assigned and unknown parameters for each step. In particular, stiffness and

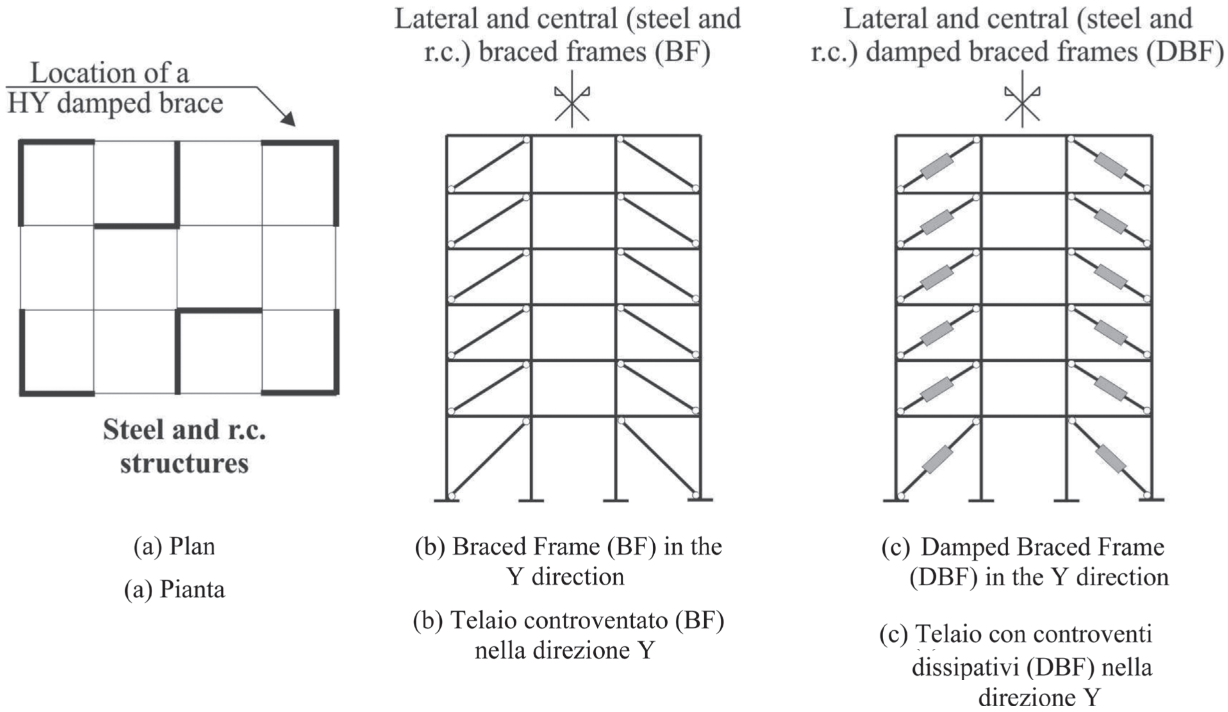

Fig. 3. *Layout of the steel and r.c. retrofitted structures.*
Schema delle strutture in acciaio ed in c.a. adeguate.

Tab. 3. *Seismic design parameters (NTC08).*
Parametri sismici di progetto (NTC08).

	a_g	T_R	F_0	S	PGA
SLD	0.094 g	50 years	2.278	1.2	0.11g
SLV	0.27 g	475 years	2.5	1.13	0.31g

Tab. 4. *Parameters of the unbraced frame (step 2.1).*
Parametri del telaio non controventato (passo 2.1).

	Assigned parameters				Unknown parameters	
	d_y (cm)	d_p (cm)	r_F	κ	$d_y^{(DB)}$ (cm)	$\xi_F^{(h)}$
Steel structure	11.83	4.82	0%	0	0.96	0
R.c. structure	2.93	3.51	0%	0.33	0.35	10.6%

Tab. 5. *Parameters of the damped brace (step 2.2).*
Parametri del controvento dissipativo (passo 2.2).

	Assigned parameters				Unknown parameters		
	μ_D	r_D	K^*_D	d_p (cm)	μ_{DB}	r_{DB}	ξ_{DB}
Steel structure	5.0	5.0%	0	4.8	4.37	5.0%	40.3%
R.c. structure	10.0	5.0%	0	3.2	8.58	5.0%	37.6%

Tab. 6. *Parameters of the damped braced frame (step 2.3).*
Parametri del telaio con controventi dissipativi (passo 2.3).

	Assigned parameters					Unknown parameters	
	ξ_V	$\xi_F^{(h)}$	ξ_{DB}	$V_y^{(DB)}$ (kN)	$V_p^{(DB)}$ (kN)	ξ_e	T_e (s)
Steel structure	5%	0	8.5%	129	155	8.5%	1.128
R.c. structure	5%	10.6%	25.1%	858	1245	25.1%	0.644

Tab. 7. *Parameters of the damped brace (step 2.4).*
Parametri del controvento dissipativo (passo 2.4).

	Assigned parameters				Unknown parameters		
	m_e ($kN \times s^2/m$)	T_e (s)	$V_p^{(F)}$ (kN)	d_p (cm)	K_e (kN/m)	$K_e^{(F)}$ (kN/m)	$K_e^{(DB)}$ (kN/m)
Steel structure	495	1.128	585	4.82	15352	12135	3216
R.c. structure	765	0.644	1315	3.51	72906	37458	35448

Tab. 8. *Parameters of the damped brace (step 2.5).*
Parametri del controvento dissipativo (passo 2.5).

	Assigned parameters				Unknown parameters	
	$K_e^{(DB)}$ (kN/m)	d_p (cm)	μ_{DB}	r_{DB}	$V_p^{(DB)}$ (kN)	$V_y^{(DB)}$ (kN)
Steel structure	3216	4.82	5.0	5.0%	155	129
R.c. structure	35448	3.51	10.0	5.0%	1245	858

strength properties of the HYDBs are reported in Tables 9a and 9b for steel and r.c. structures, respectively, assuming $K_{DB} = K_D$ in the case of *DBF* and $K_{DB} = K_B$ in the case of *BF*.

4. **Numerical Results**

A computer code was prepared to evaluate the seismic performance of steel and r.c. framed struc-

Tab. 9a. *Parameters of the HYDBs along the building height of the steel structure (step 2.6).*
Parametri dei controventi dissipativi isteretici (HYDBs) lungo l'altezza dell'edificio con struttura in acciaio (passo 2.6).

Storey	Assigned parameters				Unknown parameters	
	$V_y^{(DB)}$ (kN)	$d_y^{(DB)}$ (cm)	ϕ_i	$\cos\alpha_i$	$V_{yi}^{(DB)}$ (kN)	$K_i^{(DB)}$ (kN/m)
6	129	0.96	1.00	0.835	24	15170
5	129	0.96	0.84	0.835	57	36948
4	129	0.96	0.68	0.835	85	54777
3	129	0.96	0.52	0.835	106	68460
2	129	0.96	0.36	0.835	121	78003
1	129	0.96	0.20	0.781	129	68775

Tab. 9b. *Parameters of the HYDBs along the building height of the r.c. structure (step 2.6).*
Parametri dei controventi dissipativi isteretici (HYDBs) lungo l'altezza dell'edificio con struttura in c.a. (passo 2.6).

Storey	Assigned parameters				Unknown parameters	
	$V_y^{(DB)}$ (kN)	$d_y^{(DB)}$ (cm)	ϕ_i	$\cos\alpha_i$	$V_{yi}^{(DB)}$ (kN)	$K_i^{(DB)}$ (kN/m)
6	858	0.35	1.00	0.835	191	323318
5	858	0.35	0.83	0.835	420	589874
4	858	0.35	0.63	0.835	601	916249
3	858	0.35	0.44	0.835	731	1135712
2	858	0.35	0.26	0.835	814	1823326
1	858	0.35	0.13	0.781	858	1871235

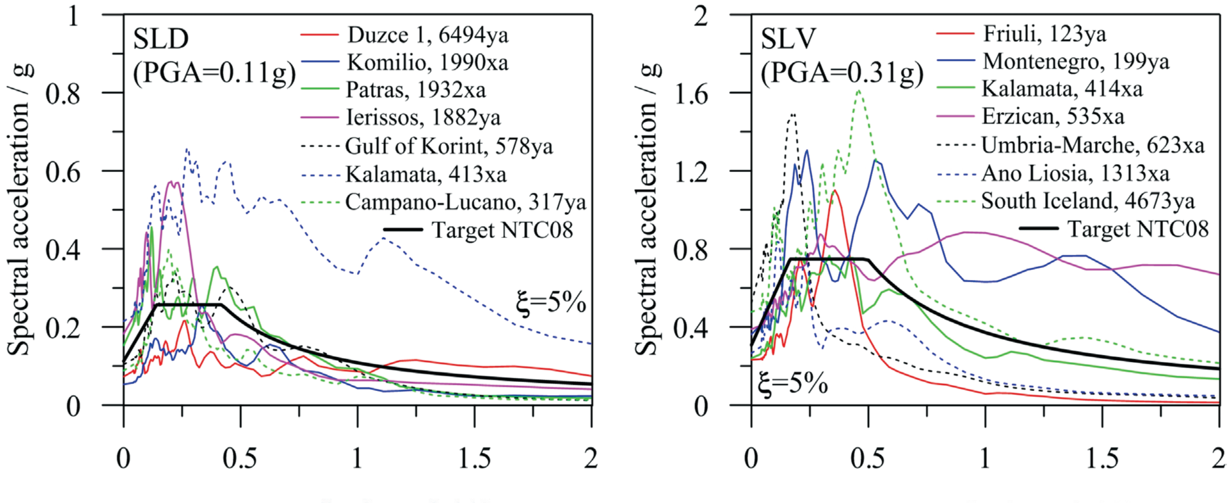

(a) Damage limit state (SLD)
(a) Stato limite di danno (SLD)

(b) Life-safety limit state (SLV)
b) Stato limite di salvaguardia della vita (SLV)

Fig. 4. *Acceleration (elastic) response spectra.*
Spettri di risposta (elastici) dell'accelerazione.

tures equipped with either steel braces or HYDBs [Mazza and Vulcano, 2007, 2010, 2011]. To this end, the frame members have been idealized by a lumped plasticity model, assuming an elastic-perfectly plastic moment-curvature law to account for the inelastic deformations at the end sections of the girders and columns [Mazza, 2014; Mazza and Mazza, 2010, 2012; Mazza and Vulcano, 2013]. The P-Δ effect and the effect of the axial load on the ultimate bending moment of the columns (M-N interaction) have also been considered, assuming fully elastic axial strains and considering, in the case of steel columns, the buckling effect. The behaviour of a HYD has been idealized by a bilinear curve while an elastic behaviour, in tension and compression, has been used for the diagonal braces, so that yielding and buckling can be prevented [Mazza and Vulcano, 2008, 2013].

A numerical investigation was carried out, evaluating the nonlinear dynamic response of the steel and r.c. original UF structures, and retrofitted BF and DBF structures subjected to real ground motions. Nonlinear dynamic analyses are carried out by a step-by-step procedure, considering two sets of seven real motions each [Iervolino et al., 2008]. These motions are selected in order to match (on average) the design spectra assumed by NTC08 for damage (Figure 4a, SLD) and life-safety (Figure 4b, SLV) limit states, taking into account the assumptions made, with regard to seismic intensity and subsoil class, in the design of the BF and DBF structures for retrofitting the UF structures. All the following results are obtained as an average of those obtained for the real motions corresponding to a limit state.

At first, the behaviour of the UF, BF and DBF steel structures is examined, checking the most critical serviceability and ultimate limit states. The maximum values of the drift ratio and horizontal displacement, induced by the SLD seismic loads, are plotted along the building height in Figure 5a and Figure 5b, respectively. The deformability thresholds imposed by NTC08

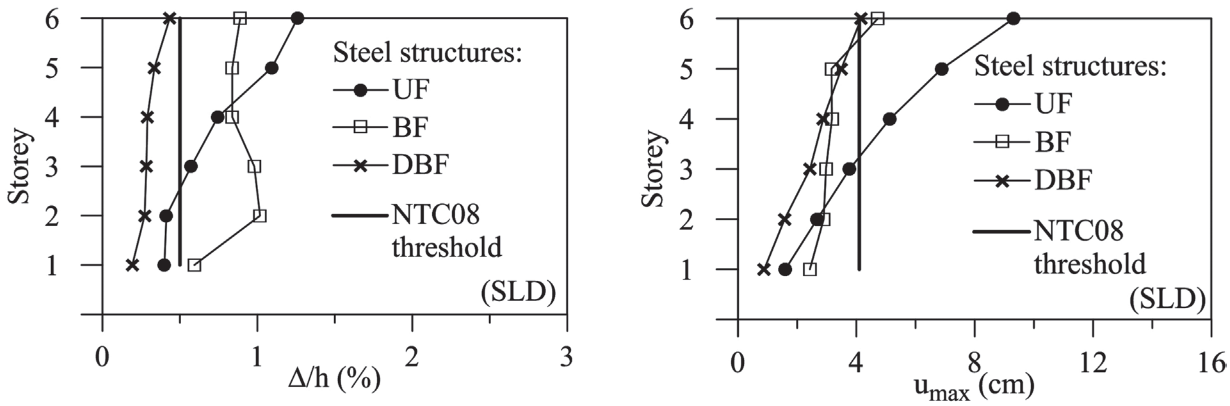

(a) Maximum drift ratio
(a) Massimo spostamento d'interpiano / altezza di interpiano

(b) Maximum displacement
(b) Massimo spostamento

Fig. 5. *Comparisons of results at the damage (SLD) limit state, obtained for the steel structures: Unbraced Frame (UF), Braced Frame (BF), Damped Braced Frame (DBF).*
Confronto fra risultati ottenuti, allo stato limite di danno (SLD), per le strutture in acciaio: telaio non controventato (UF), telaio controventato (BF), telaio con controventi dissipativi (DBF).

on the storey drift (i.e. 0.5% of the storey height) and top displacement (i.e. 1/500 of the building height) are also reported. The UF and BF structures exceed the SLD deformability thresholds at the upper storeys. On the other hand, the insertion of the HYDBs (see DBF structure) is favourable, confirming the effectiveness of their design carried out to avoid high deformability at the SLD.

Moreover, the minimum and maximum (compressive) axial loads induced by the SLV seismic loads in the more stressed column at each storey of the steel structures, are plotted in Figures 6a and 6b, respectively. As expected, the insertion of steel braces produces an increase of the axial load in comparison to that of the UF structure. Apparently, the ultimate tensile (N_{tu}) and buckling ($N_{b,Rd}$) thresholds imposed by NTC08 for the columns are not reached (mean values of minimum or maximum axial load are reported). But some analysis of BF and DBF structures has been stopped before the end of ground motion simulation, because some column buckled. In any case, the overstrength deriving from the code provisions to limit deformability and buckling led to notably reduced values of the ductility demand both for girders and columns, which remained mainly elastic.

To check the effectiveness of the BF and DBF structures for limiting the local damage undergone by the r.c. frame members, under the SLV seismic loads, in Figure 7 the maximum values of the ductility demand, calculated in terms of curvature attained at the end sections of girders (Figure 7a) and columns (Figure 7b), are shown along the frame height. As can be observed, the BF structure is unsatisfactory for seismic protection, because it increases the lateral stiffness and, due to its low damping capacity, produces an increase in the ductility demand. The insertion of the HYDBs (see DBF structure) is effective, even though columns of the second and third storeys exhibit a ductility demand slightly greater than that obtained for the UF structure.

Moreover, in order to check whether brittle failure phenomena occurred, attention was focused on the maximum values of the axial load (Figure 8a) and total shear force (Figure 8b) attained by the columns. It can be observed that the BF and DBF structures are characterized by values of the axial load in the columns higher than those in the UF structure, but the balanced compressive load (N_b) is exceeded only at the lower storeys of the BF structure. For all the structures the maximum axial load is much less than the ultimate axial load (N_{cu}). In terms of total shear forces the DBF structure proved to be more effective than the BF one, in order to stay within the value of the total shear force corresponding to the ultimate moments of the columns for the gravity loads (V_u). Further results, omitted for brevity, have confirmed the good performance of both retrofitting solutions (BF and DBF) at the SLD.

Finally, curves representing the maximum ductility demand of the HYDs, calculated as the mean of the attained maximum values at each storey under the SLD and SLV seismic loads, are plotted in Figure 9. In Figure 9, the design ductility of the dampers is also indicated: $\mu_D = 5$ for the steel structure at the SLD (Figure 9a); $\mu_D = 10$ for the r.c. structure at the SLV (Figure 9b). As can be observed, the damper ductility demands in the steel (Figure 9a) and r.c. (Figure 9b) structures are generally less than the design ductility, which is slightly exceeded only at the upper two storeys of the steel structure. These results confirm the effectiveness of the design procedure for proportioning the HYDs.

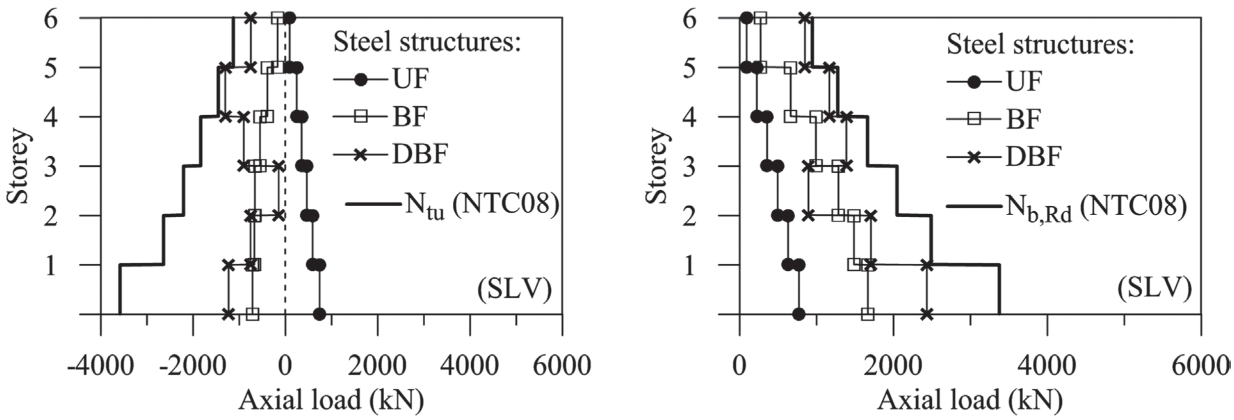

(a) Minimum axial load of columns

(a) Sforzo normale minimo dei pilastri

(b) Maximum axial load of columns

(b) Sforzo normale massimo dei pilastri

Fig. 6. *Comparisons of results at the life-safety (SLV) limit state, obtained for the steel structures: Unbraced Frame (UF), Braced Frame (BF), Damped Braced Frame (DBF).*
Confronto fra risultati ottenuti, allo stato limite di salvaguardia della vita (SLV), per le strutture in acciaio: telaio non controventato (UF), telaio controventato (BF), telaio con controventi dissipativi (DBF).

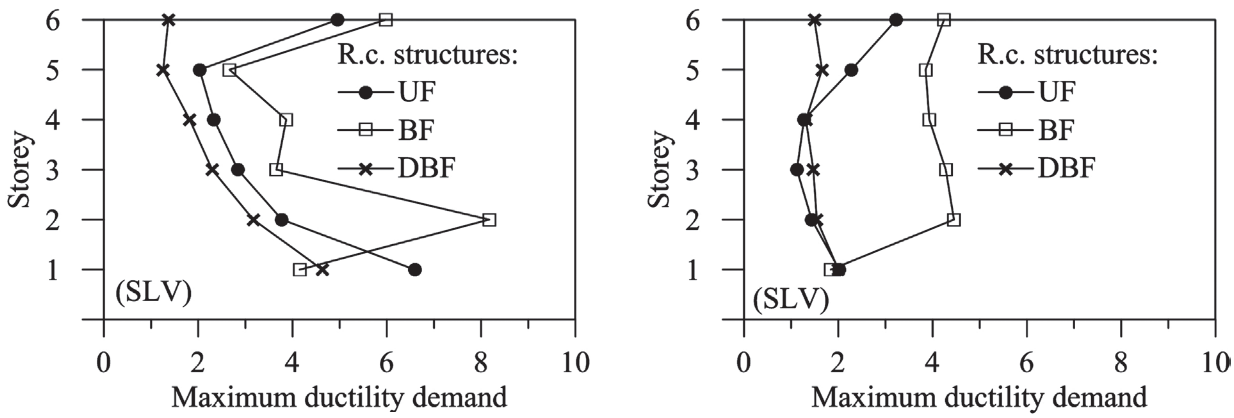

(a) Girders

(a) Travi

(b) Columns

(b) Pilastri

Fig. 7. *Comparisons of results at the life-safety limit state (SLV), obtained for the r.c. structures: Unbraced Frame (UF), Braced Frame (BF), Damped Braced Frame (DBF).*
Confronto fra risultati ottenuti, allo stato limite di salvaguardia della vita (SLV), per le strutture in c.a.: telaio non controventato (UF), telaio controventato (BF), telaio con controventi dissipativi.

5. **Conclusions**

For the purpose of retrofitting a steel-office and a r.c.-residential framed buildings from a medium- to a high-risk seismic region of the Italian classification (NTC08), diagonal steel braces acting alone (as in BF structure) or equipped with HYDs (as in DBF structure) are inserted in the original framed structure (i.e UF structure). A D.B.D. procedure has been adopted for proportioning steel braces and HYDs, to avoid high deformability of the steel structure and brittle behaviour of the r.c. structure, respectively, at the serviceability and ultimate NTC08 limit states. The results presented in this paper confirmed that the DBF steel structure, retrofitted for the damage limit state (SLD), also worked very well for the life-safety limit state (SLV), while the DBF r.c. structure, retrofitted for the SLV, was also effective for the SLD. On the contrary, the BF (steel and r.c.) structures proved always unsatisfactory for the seismic protection, because they increased the lateral stiffness of the building and, due to their low damping capacity, generally produced an increase in the (SLD) drift ratio and (SLV) ductility demand in comparison with the values obtained for the corresponding UF structures. The distribution of damper ductility demand varied along the building height, with values generally less than the design ones at SLD and SLV.

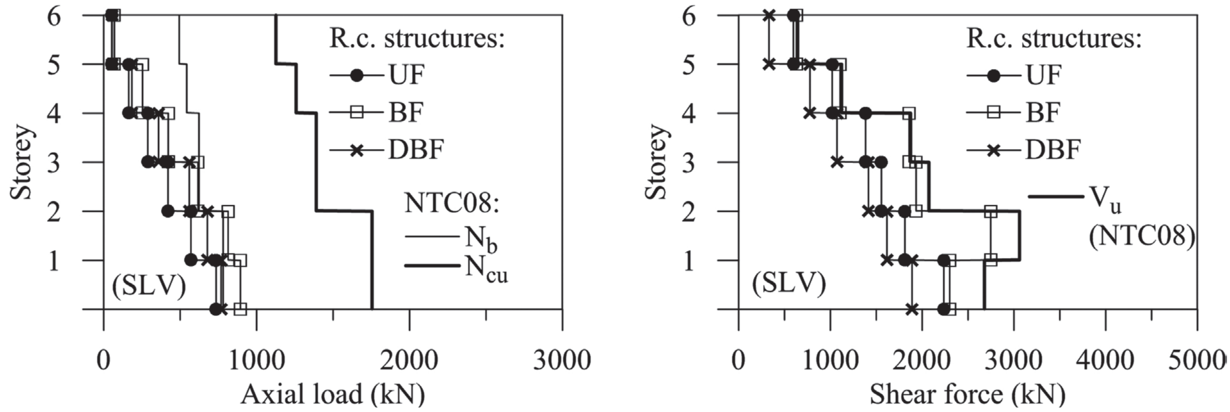

(a) Maximum axial load of columns

(a) Sforzo normale massimo dei pilastri

(b) Maximum total shear force of columns

(b) Sforzo di taglio totale dei pilastri

Fig. 8. *Comparisons of results at the life-safety limit state (SLV), obtained for the r.c. structures: Unbraced Frame (UF), Braced Frame (BF), Damped Braced Frame (DBF).*
Confronto fra risultati ottenuti, allo stato limite di salvaguardia della vita (SLV), per le strutture in c.a.: telaio non controventato (UF), telaio controventato (BF), telaio con controventi dissipativi (DBF).

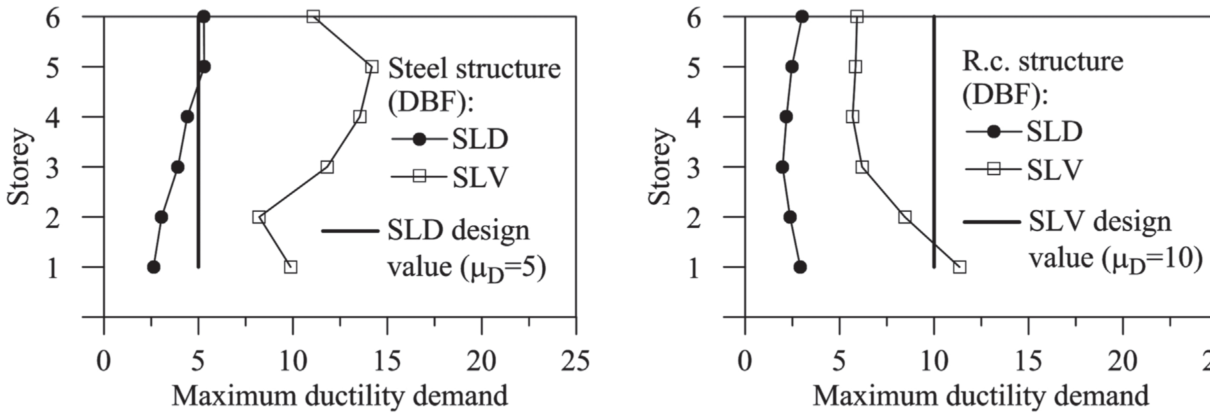

(a) HYDs of damped braced steel frame

(a) Dissipatori isteretici del telaio in acciaio con controventi dissipativi

(b) HYDs of damped braced r.c. frame

(b) Dissipatori isteretici del telaio in c.a. con controventi dissipativi

Fig. 9. *Comparisons of results at the damage (SLD) and life-safety (SLV) limit states, obtained for Hysteretic Dampers (HYDs) of Damped Braced Frame (DBF).*
Confronto fra risultati ottenuti, agli stati limite di danno (SLD) e di salvaguardia della vita (SLV), per i dissipatori isteretici (HYDs) del telaio con controventi dissipativi.

Acknowledgements

The present work was financed by Re.L.U.I.S. (Italian network of university laboratories of earthquake engineering), according to “convenzione D.P.C.-ReLUIS 2010-2013, task 2.3.2”.

References

/1/ Applied Technology Council [1996] *Seismic evaluation and retrofit of concrete buildings*, Report no. ATC 40, vol. 1, Redwood City, CA.

/2/ Bertero, VV. [2002] “Innovative approaches to earthquake engineering,” *WIT Press*, Edited by G. Oliveto, University of Catania (Italy), 1-84.

/3/ Christopoulos, C., and Filiatrault, A. [2006] *Principles of passive supplemental damping and seismic isolation*, IUSS Press, Istituto Universitario di Studi Superiori di Pavia (Italy).

/4/ DM96 [1996]. Italian Ministry of Public Works. *Norme tecniche per le costruzioni in zone sismiche e relative istruzioni*, D.M. 16-01-1996 e Circolare M.ro LL.PP. 10-04-1997, n. 65/AA.GG.

/5/ Fajfar, P. [1999] “Capacity spectrum method based on inelastic spectra,” *Earthquake Engineering and Structural Dynamics* **28**, 979-993.

/6/ Iervolino, I., Maddaloni, G., and Cosenza, E. [2008] “Eurocode 8 compliant record sets for seismic analysis of structures,” *Journal of Earthquake Engineering* **12(1)**, 54-90.

/7/ Jacobsen, L.S. [1930] "Steady forced vibrations as influenced by damping," *ASME Transaction* **52(1)**, 69-181.

/8/ Mazza, F. [2014] "A distributed plasticity model to simulate the biaxial behaviour in the nonlinear analysis of spatial framed structures," *Computers and Structures* **135**, 141-154.

/9/ Mazza, F., and Mazza, M. [2010] "Nonlinear analysis of spatial framed structures by a lumped plasticity model based on the Haar-Kàrmàn principle. *Computational Mechanics* **45**, 647-664.

/10/ Mazza, F., and Mazza, M. [2012] "Nonlinear modeling and analysis of r.c. framed buildings located in a near-fault area," *The Open Construction & Building Technology Journal* **6**, 346-354.

/11/ Mazza, F., and Vulcano, A. [2007] "Control of the along-wind response of steel framed buildings by using viscoelastic or friction dampers," *Wind & Structures* **10(3),** 233-247.

/12/ Mazza, F., and Vulcano, A. [2008] "Displacement-based seismic design procedure for framed buildings with dissipative braces. (a) Part I: Theoretical formulation; (b) Part II: Numerical results," *2008 Seismic Engineering International Conference commemorating the 1908 Messina and Reggio Calabria Earthquake (MERCEA08),* Reggio Calabria (Italy), American Institute of Physics Conference Proceedings, U.S.A, Vol. 1020 (part two).

/13/ Mazza, F., and Vulcano, A. [2009] "Nonlinear response of rc framed buildings with isolation and supplemental damping at the base subjected to near-fault earthquakes," *Journal of Earthquake Engineering* **13(5)**, 690-715.

/14/ Mazza, F., and Vulcano, A. [2010] "Nonlinear dynamic response of r.c. framed structures subjected to near-fault ground motions," *Bulletin of Earthquake Engineering* **8**, 1331-1350.

/15/ Mazza, F., and Vulcano, A. [2011] "Control of the earthquake and wind dynamic response of steel-framed buildings by using additional braces and/or viscoelastic dampers," *Earthquake Engineering and Structural Dynamics* **2**, 155-174.

/16/ Mazza, F., and Vulcano, A. [2013] "Nonlinear seismic analysis to evaluate the effectiveness of damped braces designed for retrofitting r.c. framed structures," *International Journal of Mechanics* **7(3)**, 251-261.

/17/ Mazza, F., and Vulcano, A. [2014] "Equivalent viscous damping for displacement-based seismic design of hysteretic damped braces for retrofitting framed buildings," *Bulletin of Earthquake Engineering,* DOI 10.1007/s10518-014-9601-5.

/18/ NTC08 [2008]. Italian Ministry of Infrastructures. *Nuove norme tecniche per le costruzioni e relative istruzioni*, D.M.14-01-2008 e Circolare 02-02-2009, n. 617/C.S.LL.PP.

/19/ Ponzo, F.C., Di Cesare, A., Arleo, G., and Totaro, P. [2010] "Protezione sismica di edifici esistenti con controventi dissipativi di tipo isteretico: aspetti progettuali ed esecutivi," *Progettazione Sismica* **2**, 37-60.

/20/ Ponzo, F.C., Di Cesare, A., Nigro, D., Vulcano, A., Mazza, F., Dolce, M., and Moroni, C. [2012] "JET-PACS project: dynamic experimental tests and numerical results obtained for a steel frame equipped with hysteretic damped chevron braces," *Journal of Earthquake Engineering* **16**, 662-685.

/21/ Priestley, M.J.N., Calvi, G.M., and Kowalsky, M.J. [2007] *Displacement-based seismic design of structures*, IUSS Press, Istituto Universitario di Studi Superiori di Pavia (Italy).

/22/ Sorace, S., and Terenzi, G. [2009] "Fluid viscous damper-based seismic retrofit of steel structures: general concepts and design applications," *Advanced Steel Construction*, **5**, 322-339.

/23/ Sorace, S., and Terenzi, G. [2012a] "The damped cable system for seismic protection of frame structures. Part II: Design and application," *Earthquake Engineering & Structural Dynamics*, **41**, 929-947.

/24/ Sorace, S., and Terenzi, G. [2012b] "Dissipative bracing-based seismic retrofit of R/C school buildings", *The Open Construction & Building Technology Journal*, **6**, 334-345.

Progettazione di controventi dissipativi isteretici per il miglioramento delle prestazioni sismiche di strutture intelaiate in acciaio ed in c.a.

F. Mazza, A. Vulcano

La vulnerabilità sismica delle costruzioni esistenti, in particolare di edifici con struttura intelaiata in acciaio o in c.a., è un problema molto sentito e di notevole rilevanza. In molti casi emergono livelli di rischio sismico medio-alti dovuti a carenze derivanti da una progettazione effettuata in base a normative precedenti, che, alla luce delle conoscenze attuali, risultano essere inadeguate sia nella definizione delle azioni sismiche di progetto che nella scelta delle caratteristiche strutturali e dei dettagli costruttivi. Le Norme Tecniche per le Costruzioni attualmente vigenti (NTC08) consentono l'utilizzo di controventi dissipativi ai fini dell'adeguamento antisismico delle strutture esistenti. Tuttavia, per un loro uso diffuso è essenziale disporre di procedure progettuali abbastanza semplici e al contempo affidabili, tali da poter essere agevolmente impiegate nella pratica professionale.

In linea con l'approccio prestazionale previsto dalle NTC08, è stata messa a punto una procedura per il progetto di controventi dissipativi, al fine di adeguare sismicamente edifici con struttura intelaiata in acciaio o in c.a. In particolare, la procedura di progetto proposta riguarda controventi con dissipatori di tipo isteretico, seguendo un approccio basato sul controllo degli spostamenti ("Displacement-Based Design"). Utilizzando i risultati dell'analisi statica non lineare della struttura da adeguare, i passi principali della procedura di progetto, eventualmente di tipo iterativo, sono i seguenti: (1) definizione delle caratteristiche del sistema ad 1 g.d.l. equivalente alla struttura intelaiata originaria; (2) calcolo del fattore di smorzamento viscoso equivalente per tener conto della dissipazione isteretica della suddetta struttura; (3) valutazione del fattore di smorzamento viscoso del controvento dissipativo equivalente; (4) calcolo, eventualmente iterativo, del fattore di smorzamento viscoso equivalente della struttura con controventi dissipativi; (5) calcolo del periodo fondamentale efficace della struttura con controventi dissipativi; (6) calcolo della rigidezza efficace del controvento dissipativo equivalente; (7) calcolo della resistenza del controvento dissipativo equivalente; (8) distribuzione in elevazione delle proprietà di rigidezza e resistenza dei controventi dissipativi.

L'efficacia e l'affidabilità della procedura di progetto vengono valutate considerando due edifici di sei piani, con struttura intelaiata in acciaio o in c.a., che, originariamente progettati nell'ipotesi di una regione a medio rischio sismico, devono essere adeguate per una regione ad alto rischio sismico. Per evitare eccessiva deformabilità della struttura in acciaio, allo stato limite di danno (SLD), e comportamento fragile della struttura in c.a., allo stato limite di salvaguardia della vita (SLV), si esaminano due soluzioni strutturali che prevedono l'impiego di controventi metallici diagonali senza o con dissipatori isteretici. Viene quindi svolta un'indagine numerica in regime dinamico non lineare sottoponendo le strutture considerate a gruppi di accelerogrammi reali. Più precisamente, vengono utilizzati due gruppi di sette accelerogrammi reali selezionati in modo da riprodurre (in media) lo spettro di progetto delle NTC08 agli stati limite SLD ed SLV. Tutti i risultati sono ottenuti come media di quelli ricavati, separatamente, per i gruppi di accelerogrammi corrispondenti ai due stati limite considerati.

L'analisi dinamica non lineare delle strutture considerate viene condotta seguendo una procedura al passo basata su uno schema d'integrazione nel tempo di tipo implicito, a due parametri, e su una procedura iterativa del tipo "initial-stress". Ad ogni passo dell'analisi, le condizioni di plasticità sono controllate nelle sezioni di estremità di ciascun elemento della parte intelaiata, assumendo un legame momento-curvatura di tipo bilineare, con pendenza del ramo incrudente pari al 5%. Inoltre, viene considerata l'influenza che lo sforzo normale esercita sul momento di plasticizzazione dei pilastri (interazione M-N). Il legame forza-spostamento dei dissipatori isteretici viene schematizzato mediante una legge bilineare, con pendenza del ramo incrudente pari al 5%.

I risultati ottenuti hanno confermato l'efficacia della procedura di progetto utilizzata. Per l'edificio in acciaio i controventi dissipativi, progettati allo SLD, sono risultati efficaci nel ridurre la deformabilità della struttura (in esercizio); d'altra parte, i controventi tradizionali sono risultati scarsamente efficaci allo SLD. Per l'edificio in c.a. i controventi dissipativi, progettati allo SLV, sono risultati efficaci nel ridurre la richiesta di duttilità delle travi e dei pilastri (allo stato ultimo); d'altra parte, i controventi tradizionali sono risultati scarsamente efficaci allo SLV. La procedura di progetto utilizzata si è dimostrata affidabile, consentendo di ottenere una risposta strutturale soddisfacente anche allo stato ultimo (SLV), per l'edificio in acciaio, e in esercizio (SLD), per l'edificio in c.a.